Dissociation Routes of Protonated Toluene Probed by Infrared Spectroscopy in the Gas Phase†

Detlef Schröder,*,‡,§ Helmut Schwarz,§ Petr Milko,‡ and Jana Roithová*,‡

Institute of Organic Chemistry and Biochemistry, Academy of Sciences of the Czech Republic, Flemingovo námesti 2, 16610 Praha 6, Czech Republic, and Institut für Chemie der Technischen Universität Berlin, Strasse des 17. Juni 135, D-10623 Berlin, Germany.

Received: November 30, 2005; In Final Form: April 10, 2006

The structures of $C_7H_9^+$ ions generated by protonation of toluene are investigated by means of gas-phase infrared spectroscopy in conjunction with labeling experiments and complementary mass spectrometric studies. In full consistency with previous studies, the unimolecular as well as the multiphoton-induced dissociation of mass-selected $C_7H_9^+$ ions lead to losses of molecular hydrogen and methane. Labeling data clearly imply the occurrence of skeletal rearrangements of protonated toluene to isomeric structures in the course of fragmentation. Complementary reactivity studies indicate, however, that the $C_7H_7^+$ ions generated upon dehydrogenation of $C_7H_9^+$ bear the benzylium structure, rather than that of the more stable tropylium ion. Combination of labeling data and extensive theoretical studies lead to a scheme for the fragmentation of protonated toluene, which can account for all experimental findings reasonably well. As far as infrared spectroscopy of gaseous ions is concerned, the present results confirm the structural predictions derived from theory and provide evidence for the existence of protonated cycloheptatriene but also pose some questions about the comparability of intensities in multiphoton dissociation and linear absorption spectra.

Introduction

Ever since the beginning of physical organic chemistry, protonated arenes have attracted considerable attention as intermediates in the electrophilic substitution of aromatic compounds. These so-called σ-complexes are also referred to as Wheland intermediates.[1] Notwithstanding this long interest, several of the seemingly simple properties of protonated arenes still pose fundamental challenges to chemistry. In fact, even the structure of protonated benzene has been the subject of some debate until quite recently.[2−5] As far as toluene, one of the most simple derivatives of benzene, is concerned, Kuck et al. reported already in 1985 that protonation of toluene may be associated with rearrangements to isomeric structures,[6] such as protonated cycloheptatriene, norcaradiene, and related structures which have meanwhile been elucidated in quite some detail by further experimental and theoretical investigations of Kuck and co-workers, which also included a careful evaluation of the underlying energetics.[6,7] Thus, much like neutral[8,9] and ionized[10] toluene, also protonated toluene is obviously undergoing substantial skeletal rearrangements.[11]

Here, we address the structures of $C_7H_9^+$ ions formed upon protonation of toluene in more detail using isotopic labeling as well as gas-phase infrared spectroscopy. Our specific interest in this system derives from the earlier findings of Kuck et al.,[6] which indicate that the major dissociation channels of $C_7H_9^+$, losses of H_2 as well as CH_4, show an uncoupling of these two processes with regard to the extent of H/D equilibration prior to dissociation; such a behavior is of particular interest, because it requires an unusual underlying kinetic scheme.[11−13] To investigate this aspect, we decided to combine gas-phase infrared spectroscopy with isotopic labeling experiments and adequate ab initio studies of the relevant parts of the $C_7H_9^+$ potential-energy surface.

Experimental and Computational Details

Sector-Field Mass Spectrometer. In extension to the previous work of Kuck et al.,[6] some additional labeling studies were performed using a modified VG ZAB/HF/AMD four-sector mass spectrometer of BEBE configuration (B stands for magnetic and E for electric sector).[14] Briefly, the ions of interest were generated by chemical ionization of neutral toluene isotopologs with various reagent gases, accelerated to a kinetic energy of 8 keV, mass-selected by means of B(1)/E(1), and the unimolecular fragmentations of metastable ions (MI) occurring in the field-free region preceding the second magnet were monitored by scanning B(2). As reagent gases in chemical ionization, hydrogen, water, isobutane, and ammonia were used. All spectra were accumulated with the AMD-Intectra data system; 5−15 scans were averaged to improve the signal-to-noise ratio. Final data were derived from two to five independent measurements with an experimental error smaller than ±2% for most channels. In the case of the mass differences $\Delta m = -1$ and -2, however, the data for protonated toluene need to be corrected for unimolecular H (D) losses from the ^{13}C contribution of the molecular ion of toluene (and the isotopologs),[15] which increases the errors to about ±10% in these particular two channels.

ICR Experiments. The ion-cyclotron resonance (ICR) experiments were performed with a compact ICR instrument[16] mounted to the beam line of a free electron laser at CLIO (Centre Laser Infrarouge Orsay, France). Briefly, the ions of interest were generated by means of the following sequence. First, a pulse of a suitable reagent gas was admitted to the mass spectrometer, in whose maximum an electron−ionizer was

† Part of the "Chava Lifshitz Memorial Issue".
‡ Academy of Sciences of the Czech Republic.
§ Institut für Chemie der Technischen Universität Berlin.

10.1021/jp056962f CCC: $33.50
Published on Web 05/16/2006

switched on for about 0.3 s, thereby establishing a chemical ionization plasma. This first step is followed by a pulse of toluene (or an isomeric C_7H_8 compound) and mass-selection of so-formed $C_7H_9^+$ ions using double-resonance techniques. The C_7H_8 pulses were kept as short as possible to minimize secondary reactions, as probed by monitoring of degenerate proton transfer with the labeled ions as well as the methylene-transfer reaction of benzylium ions (see below). These control experiments establish that secondary reactions with neutral C_7H_8 were negligible. Subsequently, infrared multiphoton dissociation (IRMPD) was induced by admittance of laser light to the ICR cell for about a second. In the 40−45 MeV range in which CLIO was operated in these experiments, the IR light covers a range from about 1000 to 1700 cm^{-1}. Effects of laser wavelength and flux, laser-power dependence, and irradiation time were checked for respective control experiments, and unless mentioned otherwise, no dependences other than expected were found.[17]

Theoretical Methods. All calculations reported were performed using the density functional method B3LYP[18−20] in conjunction with triple-ζ basis sets 6-311+G(2d,p) as implemented in the Gaussian 98 package of programs.[21] Frequency analysis at the same level of theory established all optimized structures as genuine minima or transition structures on the potential-energy surface. In addition, the computed harmonic frequencies were used to calculate zero-point vibrational energy (ZPVE); for comparison with the experimental infrared data, the frequencies were scaled by 0.96. The relative energies (E_{rel}) mentioned below refer to 0 K and are given in electronvolts relative to the most stable isomer, para-protonated toluene.

Results and Discussion

The dissociation of mass-selected $C_7H_9^+$ cations has first been studied by Hvistendahl and Williams,[22] who examined the unimolecular dehydrogenation of dihydrotropylium ions and argued that tropylium is formed as ionic fragment due to conservation of orbital symmetry. The potential-energy surface of $C_7H_9^+$ ions then later received quite some attention in the context of the reaction of CH_3^+ cations with benzene.[23] Particularly detailed studies of Kuck and co-workers addressed the dissociation of protonated toluene using sophisticated labeling techniques[6] and various $C_7H_9^+$ ions of alternative structures.[7] Recently, $C_7H_9^+$ ions obtained upon protonation of toluene were characterized by gas-phase infrared spectroscopy,[24] and another recent work on $C_7H_9^+$ ions used gas-phase titration experiments to estimate the contributions of several $C_7H_9^+$ isomers when the ions are made via different routes.[7e]

Our particular interest in $C_7H_9^+$ arises from the following considerations. (i) The earlier results of Kuck and co-workers[6,7,11] reveal that the two major dissociation channels (H_2 and CH_4 losses) both show extensive isotope scrambling (of hydrogen as well as carbon atoms), thereby implying the occurrence of skeletal rearrangements prior to dissociation. (ii) The extent of isotope scrambling in H_2 and CH_4 losses appears to be different, thereby indicating that the channels are at least to some extent uncoupled from each other. (iii) The $C_7H_9^+$ system should be well-suited to probe the ability of gas-phase infrared spectroscopy for a distinction of isomeric ions in general and even more so in the particular case when these isomers may be able to interconvert into each other. (iv) Last but not least, the underlying reaction mechanisms and the possible isomerization pathways of protonated toluene prior to fragmentation and the associated kinetic schemes are of interest.

To illustrate the complexity of the problems associated with the dissociation of $C_7H_9^+$, let us briefly discuss the fragmentation

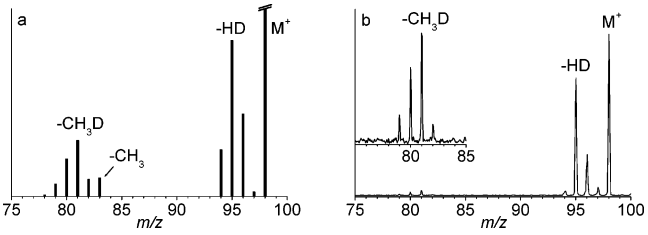

Figure 1. (a) Relative fragment-ion abundances formed upon unimolecular dissociation of mass-selected $C_7H_4D_5^+$ ions ($m/z = 98$) generated by chemical ionization of $C_6D_5CH_3$ using H_2O as reagent gas in a sector-field mass spectrometer. Note that the fragments at $m/z = 96$ and 97 are corrected for the unimolecular decay of the interfering ^{13}C-contribution of the molecular ion $C_6D_5CH_3^+$. (b) Infrared multiphoton dissociation (at 1430 cm^{-1}) of mass-selected $C_7H_4D_5^+$ generated by chemical ionization of $C_6D_5CH_3$ using H_2O as reagent gas in an ion-cyclotron resonance mass spectrometer. The inset shows the C_1 losses with a magnification factor of 30.

pattern of the $C_7H_4D_5^+$ species obtained upon protonation of ring-deuterated toluene ($C_6D_5CH_3$). At this stage, we would like to point out clearly, however, that our interest is neither the process of protonation itself nor an even more detailed analysis of the fragmentation patterns than that already performed before,[6,7] but to first point out the fundamental differences between the $C_7H_4D_5^+$ ions sampled in both experiments. Figure 1 shows two different tandem mass spectra of $C_7H_4D_5^+$ ions ($m/z = 98$). Figure 1a summarizes the results of metastable-ion (MI) spectra for mass-selected $C_7H_4D_5^+$ obtained in a large-scale sector-field mass spectrometer, and Figure 1b shows the infrared multiphoton-dissociation (IRMPD) of $C_7H_4D_5^+$ ions trapped in an ion-cyclotron resonance mass spectrometer upon irradiation with an IR laser beam. Qualitatively, the MI and IRMPD spectra bear several similarities: Dehydrogenation prevails over loss of C_1 fragments, and for both kinds of fragmentations, the most abundant isotopologs correspond to HD and CH_3D losses, respectively. Upon more detailed inspection, however, a number of quite substantial differences become obvious. Thus, the ratio between H_2 and D_2 losses differs largely between Figure 1a,b in that significantly more D_2 loss is observed in the MI spectrum. Formation of D_2 from protonated $C_6D_5CH_3$ indicates an extensive H/D equilibration in the ion prior to dissociation, which can be due to either sampling of particularly long-lived species in the metastable-ion experiments or a high average content of internal energy that allows for more extensive rearrangements (see below). Further, both figures show ratios of H_2, HD, and D_2 losses that are far from the 3:10:5 pattern expected for a fully statistical isotope distribution. Even more puzzling is the fact that despite the considerable H/D equilibration in the dehydrogenation channel, the elimination of methane preferentially involves the intact CH_3 group of the neutral precursor in that CH_3D loss predominates in both experiments,[6] whereas CH_2D_2 should largely be favored in the case of statistical equilibration, for which CH_4:CHD_3:CH_2D_2:CHD_3:CD_4 = 1:20:60:40:5 is expected. We further note that the sector-field experiments also reveal small, but nonnegligible, amounts of fragmentations corresponding to the expulsion of open-shell neutrals from the closed-shell ion $C_7H_9^+$, namely, $H^\bullet$ as well as $CH_3^\bullet$ (and their isotopologs); likewise, a small signal at $m/z = 97$ is observed in the IRMPD spectrum. Hence, the dissociation of $C_7H_9^+$ involves two competing major channels (H_2 and CH_4 losses) in which different amounts of scrambling take place, thereby indicating a quasi-irreversible contribution in the competition of both processes. This pattern is further complicated by two associated minor pathways ($H^\bullet$ and $CH_3^\bullet$ losses). Because of the overlapping $D^\bullet$ and H_2 losses

TABLE 1: Relative Abundances of H_2, HD, CH_4, and CH_3D Losses upon IRMPD of Mass-Selected $C_7H_8D^+$ Generated by Chemical Ionization of the Neutral Precursors and Reagent Gases Indicated

	toluene, C_3D_8	toluene, D_2O	CHT,[a] D_2O
$-H_2$[b]	93	81	78
$-HD$[b]	4	9	13
$-CH_4$[b]	2	6	4
$-CH_3D$[b]	1	4	5
$x(C_7H_8D^+)$[b,c]	0.51	0.45	0.53

[a] CHT stands for cycloheptatriene. [b] Branching ratios and conversion have an experimental error of ±1%. [c] Molar fraction of the parent ions, which do not undergo photofragmentation, is given for comparison in terms of the conversion $x(C_7H_8D^+) = I(C_7H_8D^+)/\Sigma I_i$.

(both $\Delta m = 2$ amu), also a concise deconvolution of the isotope patterns for an adequate set of isotopically labeled precursors[12,13,25] turned out to be impossible.

Next, the influence of ion generation on the MS/MS spectra is considered. In the metastable-ion studies conducted in the sector-field experiment, no significant influence of the ionization conditions on the fragmentation patterns of mass-selected, metastable $C_7H_{9-n}D_n^+$ ions was found. In particular, the MI spectra were independent of the reagent gas used in chemical ionization, i.e., hydrogen, water, isobutane, and ammonia. This result is after all not surprising, however, because metastable-ion experiments do not sample different decay rates of ions having identical internal energies relative to the common precursor, but similar dissociation rates of ions having different internal energies.[26] Thus, upon protonation with Brønsted acids of increasing strength the $C_7H_9^+$ ions will decay faster, but the fractions of reacting ions sampled in the metastable-ion experiments remain more or less identical.

In contrast, the IRMPD data show a slight, yet clear, dependence from the ionization conditions. For illustration of this effect, one is referred to monodeuterated $C_7H_8D^+$ as an example (Table 1). When C_3D_8 is used as the reagent gas, the initial ionization processes primarily lead to $C_3D_7^+$, as a Brønsted acid of moderate strength, i.e., $PA(C_3H_6) = 7.74$ eV compared to PA(toluene) = 8.06 eV.[27] Hence, the $C_7H_8D^+$ species can be assumed to be formed with a only very moderate excess of internal energy. IRMPD of so-formed $C_7H_8D^+$ leads to a large preference for H_2 loss. In contrast, use of D_3O^+ as a stronger Brønsted acid ($PA(H_2O) = 7.11$ eV) significantly increases the fraction of HD elimination, also accompanied by increased demethanation. Thus, the larger amount of internal energy deposited upon protonation increases the efficiency of H/D exchange and also enforces the loss of C_1 fragments. Interestingly, similar results are obtained with cycloheptatriene as the neutral precursor in that even still less selective H_2 elimination is observed, whereas demethanation is of similar total abundance. The fact that the ratio of CH_4 and CH_3D losses is inverted from toluene to cycloheptatriene might first appear surprising, but it finds a clear rationale in the selective participation of the methyl group in the case of toluene,[6] whereas all H/D atoms can safely be assumed to be equilibrated prior to loss of C_1 fragments from protonated cycloheptatriene. Note that the preferential loss of CH_3D, rather than CH_4, from the $C_7H_8D^+$ ion generated from cycloheptatriene can be explained by an isotope effect in favor of H migration.

Let us now address the role of the wavelength and the power of the infrared irradiation. In the frequency range studied (1000−1700 cm^{-1}), the $C_7H_9^+$ ions investigated here have three major absorption bands at about 1250, 1450, and 1590 cm^{-1}, of which the middle one is most intense. These spectral features are discussed in more detail further below, but prior to this analysis, the fragmentation pattern shall be considered. By and large, our results confirm the previous findings of Kuck et al. and Dopfer et al. as far as product and labeling patterns of H_2 and CH_4 losses are concerned.[6,24] We note, however, that the loss of methane is sensitive to the experimental conditions in that the fraction of C−C cleavage can range up to 10% of the total fragmentation but may also almost vanish under certain conditions.

TABLE 2: Branching Ratio for Dehydrogenation and Loss of Methane upon IRMPD of Mass-Selected $C_7H_9^+$ at Three Different Absorption Maxima

	1250 cm^{-1}	1450 cm^{-1}	1590 cm^{-1}
$-H_2$[a]	95	91	96
$-CH_4$[a]	5	9	4
$x(C_7H_9^+)$[a,b]	0.39	0.15	0.47

[a] Water was used as a reagent gas in CI and toluene served as a neutral precursor. Branching ratios and conversion have an experimental error of ±1%. [b] Molar fraction of the parent ion that does not undergo photofragmentation given for comparison as the conversion $x(C_7H_9^+) = I(C_7H_9^+)/\Sigma I_i$.

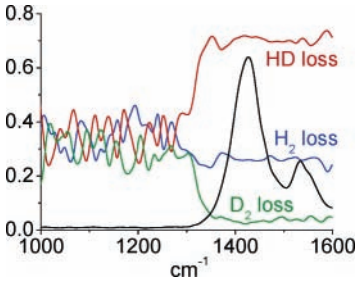

Figure 2. IRMPD spectrum (black) of mass-selected $C_7H_4D_5^+$, generated by chemical ionization of $C_6D_5CH_3$ using H_2O as reagent gas, and the separate branching ratios between H_2 (blue), HD (red), and D_2 (green) losses as a function of wavelength. At the absence of photofragmentation (below ca. 1300 cm^{-1}), the branching ratios reflect the background signals and thus scatter about 1/3.

Table 2 shows the results for three representative IRMPD mass spectra of $C_7H_9^+$ ions. Upon irradiation in the most intense absorption maximum at 1450 cm^{-1}, about 85% of the incident ions undergo photofragmentation, whereas significantly less fragmentation occurs in the two weaker bands at 1250 and 1590 cm^{-1}, clearly highlighting the role of multiphoton processes. Parallel with the amount of fragmentation, also the branching for CH_4 loss increases slightly, but significantly at 1450 cm^{-1}; similar conclusions can be derived from the experiments of Dopfer et al. in that CH_4 loss is most pronounced in the most intense IR bands.[24] Wavelength dependences of the branching ratios in competing reactions upon IRMPD have been mentioned previously but were either attributed to consecutive processes or neglected within the experimental error margins.[17,28,29] In the present case, however, the dependence of the methane loss from the amount of energy absorbed by the $C_7H_9^+$ ions is obvious. Moreover, the observed increase of the methane loss with increasing absorption is fully consistent with the effect observed for stronger Brønsted acids used in protonation.

In marked contrast to the branching between C−H- and C−C-bond activation, the isotope pattern for dehydrogenation of $C_7H_4D_5^+$ is wavelength-independent (Figure 2). The black trace in Figure 2 shows the IR spectrum of mass-selected $C_7H_4D_5^+$ generated by protonation of $C_6D_5CH_3$ with H_3O^+. Whereas unlabeled $C_7H_9^+$ has three absorption features in the spectral range investigated here (see above), the labeled ion lacks the band at about 1250 cm^{-1}, which has been attributed to the disappearance of free CH_2 scissor modes upon deuteration.[24,30] In the lack of absorbance, no photofragmentation takes place,

CHART 1: Computed Structures 1^+-21^+ of $C_7H_9^+$ Isomers (Only Singlets Shown)

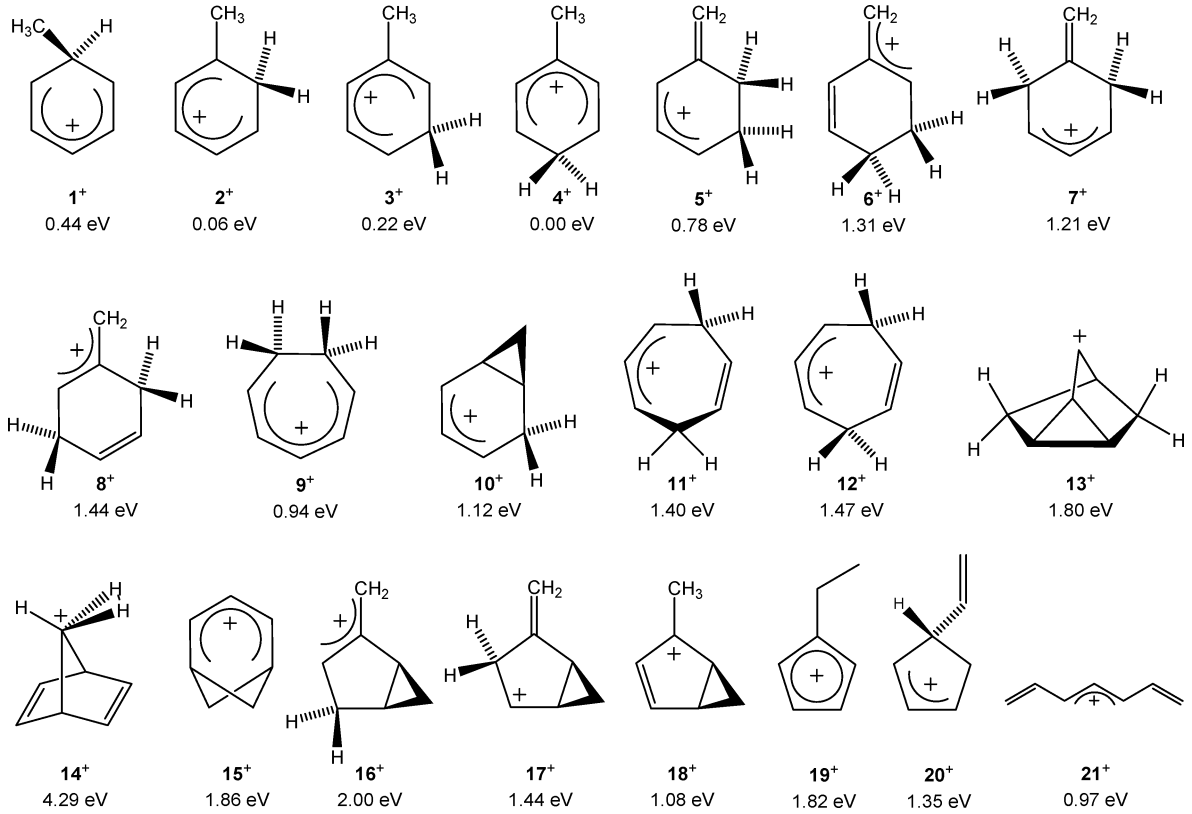

such that the colored traces, which stand for the losses of H_2, HD, and D_2, respectively, scatter around 1/3, whereas they rapidly reach plateau values of 26:71:3, once IR absorption (black line) begins without showing any apparent dependence on the wavelength of the IR photons.

Last but not least, it remains to be assessed which product ions are formed. Whereas on thermochemical grounds the loss of methane from $C_7H_9^+$ can safely be assumed to lead to the phenylium ion, dehydrogenation can afford either benzylium (**Bz**$^+$) or, after ring-expansion, the more stable tropylium ion (**Tr**$^+$). In this context, benchmark studies of Dunbar[31] and Ausloos[32] have outlined a clear-cut way to probe the ion structures by means of ion/molecule reactions. Thus, **Bz**$^+$ reacts with arenes under formal transfer of a methylene group, whereas **Tr**$^+$ is unreactive. In the particular case of toluene as a neutral reagent, the benzylium structure can be identified by the occurrence of reaction 1.

$$\underset{m/z\ 91}{C_6H_5CH_2^+} + C_6H_5CH_3 \rightarrow \underset{m/z\ 105}{CH_3C_6H_4CH_2^+} + C_6H_6 \quad (1)$$

Accordingly, the following experiment was designed to probe the structure of the photofragment ions. Neutral toluene was first protonated in a CI plasma made from isobutane followed by mass-selection of $C_7H_9^+$, which was then subjected to IRMPD and the resulting ions were allowed to interact with pulsed-in toluene. If only the more stable **Tr**$^+$ were formed upon IRMPD, no signal at $m/z = 105$ is expected at all, whereas complete conversion would imply the exclusive presence of **Bz**$^+$. The corresponding data, given in Table 3, very much support the latter scenario in that almost no unreactive fraction of $C_7H_7^+$ ions remains after a sufficiently long gas pulse of neutral toluene.

Even more remarkably, also the $C_7H_7^+$ fragment formed upon IRMPD of $C_7H_9^+$ generated by protonation of cycloheptatriene reacts with neutral toluene to afford $C_8H_9^+$ without any evidence for an unreactive fraction. Hence, it is concluded from these monitoring experiments that protonation of toluene as well as cycloheptatriene led to either the same ionic species or different $C_7H_9^+$ ions, but both yield the less stable dehydrogenation product **Bz**$^+$ upon IRMPD.

TABLE 3: Relative Abundances of $C_7H_7^+$ and $C_8H_9^+$ Ions Formed upon IRMPD of Mass-Selected $C_7H_9^+$, Followed by a Gas Pulse of Neutral Toluene with Variable Lengths.[a]

	isolation[b]	no pulse	3 s pulse	6 s pulse	12 s pulse
$C_7H_7^+$ (m/z 91)[c]	0	44	24	13	1
$C_7H_9^+$ (m/z 93)[c]	100	56	53	54	57
$C_8H_9^+$ (m/z 105)[c]	0	0	23	33	42
$x(C_7H_7^+)$[c,d]		1.00	0.49	0.28	0.03

[a] The $C_7H_9^+$ precursor ion was generated by CI of toluene using isobutane as the reagent gas. To a first approximation, the length of the gas pulse corresponds to the amount of toluene admitted to the ICR cell; a strict correlation cannot be made, however. [b] Abundances directly after mass selection of $C_7H_9^+$. [c] Branching ratios and conversion have an experimental error of ±1%. [d] Molar fraction of the $C_7H_7^+$ photofragment and its putative ionic product according to reaction 1; defined as $x(C_7H_7^+) = I(C_7H_7^+) + I(C_8H_9^+)$.

Theoretical Results. Several facets of the $C_7H_9^+$ surface have been reported in earlier theoretical studies,[7,24,33] which we complement here by a somewhat more comprehensive theoretical investigations of those $C_7H_9^+$ species related to the dissociation of protonated toluene (Chart 1). Figure 3 shows the low-lying isomers directly accessible upon protonation of toluene and cycloheptatriene, respectively. Among the protonated toluenes $\mathbf{1}^+-\mathbf{4}^+$, as expected, the para-isomer is most stable ($E_{rel} = 0.00$ eV), the ortho-form is only little more demanding ($E_{rel} = 0.06$ eV), the meta-isomer is just 0.22 eV higher in energy, and even ipso-protonated toluene is relatively low in energy.[11,24] Moreover, the barriers associated with hydrogen-ring walk are rather low in energy such that interconversion between the ring-protonated forms can be expected

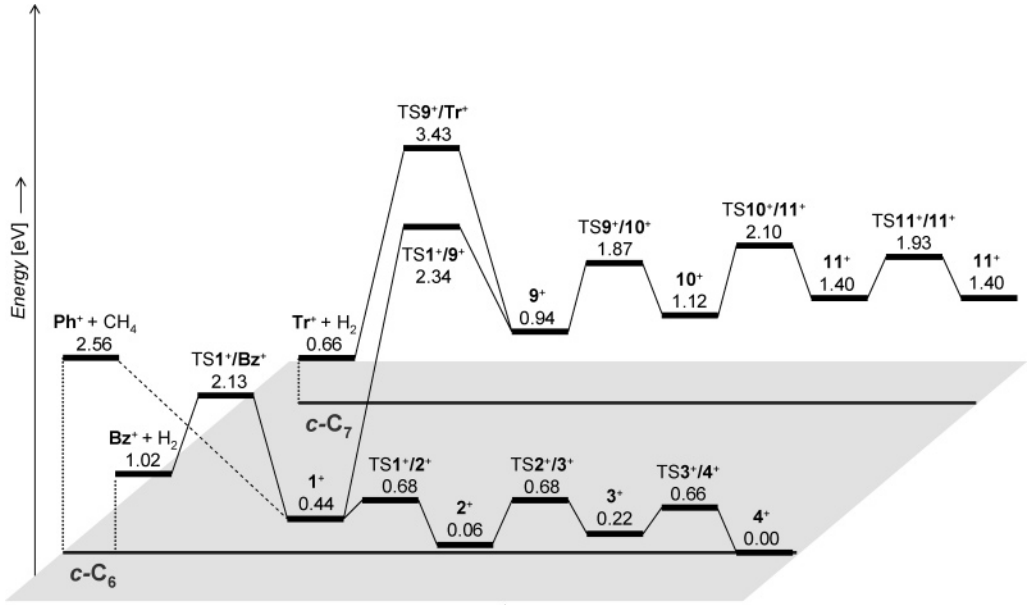

Figure 3. Potential-energy surface (eV) of the $C_7H_9^+$ isomers directly accessible upon protonation of toluene and cycloheptatriene, respectively, computed at the B3LYP/6-311+G(2d,p) level of theory.

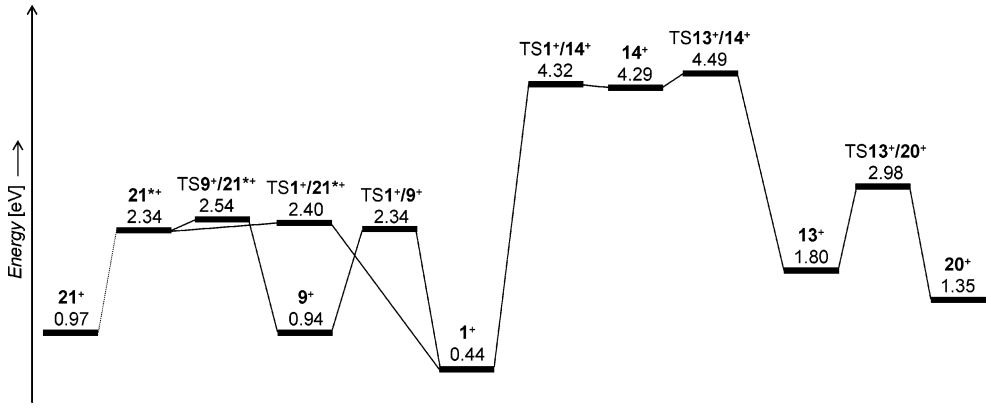

Figure 4. Potential-energy surface (eV) of other related $C_7H_9^+$ isomers computed at the B3LYP/6-311+G(2d,p) level of theory. Structure **21***+ stands for a high-energy *cisoid* conformer that is initially formed upon ring-opening of $\mathbf{9}^+$.

to easily occur at elevated energies.[11] In marked contrast, the elimination of dihydrogen to yield benzylium ion requires passage of the transition structure TS $\mathbf{1}^+/\mathbf{Bz}^+$ with $E_{rel} = 2.13$ eV, which is more than 1 eV above the final products $\mathbf{Bz}^+ + H_2$. For the latter, the B3LYP computations predict $E_{rel} = 1.02$ eV compared to an experimental value of 0.99 ± 0.05 eV.[27,34] The loss of methane, i.e., the $\mathbf{Ph}^+ + CH_4$ channel, is even somewhat more energy demanding ($E_{rel} = 2.56$ eV; exp 2.62 $\pm$ 0.06 eV[34,35]); all attempts to locate a barrier for this dissociation were unsuccessful (see below).

The interconversion to the manifold of isomers derived from protonation of cycloheptatriene also occurs from the ipso-isomer $\mathbf{1}^+$ and involves a barrier energetically situated between these two exit channels (TS $\mathbf{1}^+/\mathbf{9}^+$ with $E_{rel} = 2.34$ eV). Of the protonated cycloheptatrienes, the 1-protonated form, viz. cyclohepta-2,4-dienylium, is the most stable isomer situated 0.94 eV above para-protonated toluene $\mathbf{4}^+$. Much like for protonated toluene, the various tautomers of the seven-membered ring system ($\mathbf{9}^+-\mathbf{11}^+$) are separated by only modest barriers compared to the height of TS $\mathbf{1}^+/\mathbf{9}^+$. Interestingly, the barrier associated with dehydrogenation, TS $\mathbf{9}^+/\mathbf{Tr}^+$, is much above all species considered so far ($E_{rel} = 3.43$ eV), even though it leads to the most stable fragment ions, $\mathbf{Tr}^+ + H_2$ with $E_{rel} = 0.66$ eV (exp. 0.52 ± 0.05 eV). With respect to structures $\mathbf{9}^+$ and $\mathbf{10}^+$, we note some discrepancy to the previous work of Kuck and co-workers[7b,e] in that we find $\mathbf{9}^+$ to be 0.18 eV below $\mathbf{10}^+$, rather than the opposite; except the energetic location of $\mathbf{9}^+$, all relative energetics agree reasonably well, however.

In addition to the isomers directly derived from either toluene or cycloheptatriene, some other conceivable structures as well as their possible rearrangements were explored (see $\mathbf{12}^+-\mathbf{21}^+$ in Chart 1). As none of these species appears to be easily accessible from the precursors of interest in the present context, we thus did not pursue them any further.[36] However, it is noteworthy that the acyclic form $\mathbf{21}^+$ is by no means out of range as far as mere thermochemistry is concerned; nevertheless, the barriers en route to ring-opening are large (Figure 4).

Fragmentation Scheme of $C_7H_9^+$ Ions Generated upon Protonation of Toluene. Combining the present and all previous experimental and theoretical findings, an internally consistent picture of the fragmentation of $C_7H_9^+$ can be proposed. Of the species investigated here, the most stable ones are the protonated toluenes $\mathbf{1}^+-\mathbf{4}^+$ with the para-isomer $\mathbf{4}^+$ as the lowest-lying one ($E_{rel} = 0.00$ eV); $\mathbf{4}^+$ can also be assumed to constitute the global minimum of the $C_7H_9^+$ surface. The barriers computed for hydrogen ring-walk connecting isomers $\mathbf{1}^+-\mathbf{4}^+$ are rather low compared to those associated with all other isomerization or fragmentation pathways.[11] Accordingly, complete equilibration of all H or D atoms directly attached to the arene ring can

be assumed safely; note, however, that the assumed equilibration does not in turn, by no means, exclude the operation of a significant isotope effect in the ion fragmentation. The energetically lowest-lying pathway for dehydrogenation evolves from ipso-protonated toluene $\mathbf{1}^+$ ($E_{rel} = 0.44$ eV) and proceeds via the energy-demanding TS $\mathbf{1}^+/\mathbf{Bz}^+$ ($E_{rel} = 2.13$ eV), from which the benzylium ion is then formed. Given the height of the barrier relative to the isomers of protonated toluene and the low barriers between the latter, a significant kinetic shift is therefore to be expected in the time scale of the experiments. Moreover, particularly for ions derived from arenes, radiative stabilization may be significant[37] and thereby compete with ion fragmentation. With respect to IRMPD experiments, photon emission would effectively reduce the heating rate of the ion in the laser pulse.

As mentioned above, with the theoretical methods employed we could not locate a TS for the loss of methane from $C_7H_9^+$, which is, however, of limited relevance when the reverse process is considered. Thus, it is well-known that the phenylium ion $C_6H_5^+$ reacts with methane to afford $C_7H_7^+$ (reaction 2)

$$C_6H_5^+ + CH_4 \rightarrow C_7H_7^+ + H_2 \qquad (2)$$

with a rate constant in the order of $(7.5 \pm 2.2) \times 10^{-11}$ cm^3 s^{-1}, corresponding to about $7 \pm 2\%$ of the gas kinetic collision rate.[38] The entrance barrier associated with reaction 2 can thus safely assumed to be low; in fact, the reaction most likely occurs as a quasi-barrierless process in analogy to the reaction of phenylium ion with dihydrogen.[39] Accordingly, dehydrogenation of $C_7H_9^+$ involves the lowest-lying exit channel, but an energetically and entropically demanding TS, whereas loss of CH_4 requires somewhat more energy but is likely to compete with H_2 loss, once the former is energetically accessible.[40] This scenario can account quite well for the variation in the amount of C_1 fragments discussed above, and also nicely matches the different kinetic releases associated with both processes.[6]

Furthermore, the tropylium manifold provides a conceivable route in which the H(D) atoms of the methyl group can participate in H/D equilibration. The access to these isomers via TS $\mathbf{1}^+/\mathbf{9}^+$ ($E_{rel} = 2.34$ eV) is energetically situated between the competing channels of dehydrogenation and loss of methane, thereby offering a clear guideline for the explanation of the experimentally observed labeling patterns. Last but not least, also the large energy demand computed for the dehydrogenation to yield tropylium (TS $\mathbf{9}^+/\mathbf{Tr}^+$ with $E_{rel} = 3.43$ eV) is in perfect agreement with the experimental observation that the $C_7H_7^+$ photofragments bear the benzylium structure rather than that of the energetically more stable tropylium ion.

Infrared Spectroscopy

What remains to be considered are the infrared spectra of the $C_7H_9^+$ ions. In general, the present results are in good agreement with those previously obtained by IRMPD as far as peak positions and isotope shifts are concerned. By comparison with calculated IR spectra, these features were ascribed to the ortho- and para-isomers of protonated toluene.[24] Therefore, of the more than a dozen spectra we recorded for various isotopomers and experimental conditions, here we would like to focus on only three specific IRMPD spectra of $C_7H_9^+$ ions generated under different conditions.

Figure 5a shows the IRMPD spectrum of $C_7H_9^+$ ions generated from toluene under the softest conditions, i.e., CI plasma of isobutane. The spectrum displays the above-mentioned three major absorptions at about 1250, 1450, and 1590 cm^{-1}

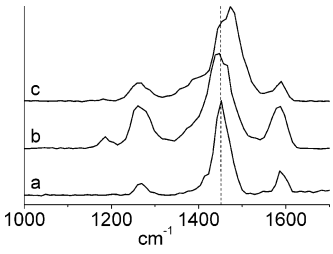

Figure 5. IRMPD spectra between 1000 and 1700 cm^{-1} of mass-selected $C_7H_9^+$ generated by chemical ionization of (a) toluene with isobutane as reagent gas, (b) toluene with water as reagent gas, and (c) cycloheptatriene with water as reagent gas.

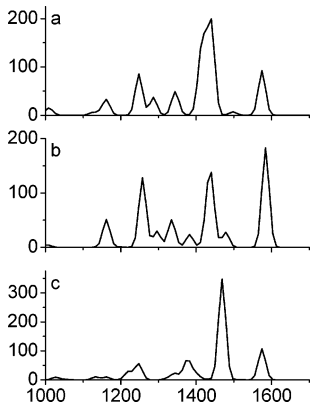

Figure 6. Calculated IR spectra between 1000 and 1700 cm^{-1} of (a) ortho-protonated toluene $\mathbf{2}^+$, (b) para-protonated toluene $\mathbf{4}^+$, and (c) 1,2-protonated cycloheptatriene $\mathbf{9}^+$ as predicted by the B3LYP calculations. As far as the positions of the resonances are concerned, a good match of the three major peaks in the experimental IRMPD spectrum is obtained,[24] whereas intensities differ substantially.

with the middle one being most intense. The spectrum obtained upon more exothermic protonation (Figure 5b) is identical to, as far as peak positions are concerned, but differs from that in Figure 5a in terms of intensities in that the weaker bands are much more pronounced. In fact, even a fourth band at about 1190 cm^{-1} is clearly visible in Figure 5b. A second notable difference concerns peak shapes in that the half widths in the order of 40 cm^{-1} in Figure 5a increase to about 70 cm^{-1} in Figure 5b in conjunction with a tailing to lower wavenumbers. This behavior is precisely what is expected for a "hot" population of ions due to the more exothermic protonation. With cycloheptatriene as a neutral precursor, the spectrum is again quite similar, yet the central band in Figure 5c now appears to have two components.

For comparison let us now consider the computed IR spectra of the most stable isomers of protonated toluene, $\mathbf{2}^+$ and $\mathbf{4}^+$, as well as that of 1,2-protonated cycloheptatriene, $\mathbf{9}^+$, in the relevant spectral region (Figure 6). As far as the positions of the bands are concerned, nicely matching IR features are observed for all three isomers in comparison to the experimental spectra. More careful inspection reveals a number of significant discrepancies, however. At first, irrespective of which isomer is considered (this also holds true for the other structures shown in Chart 1), the computed spectra show much more absorption bands than observed in experiment. For the situation in $C_7H_9^+$ isomers, one would precisely expect the opposite, however, in that the similar stabilities of $\mathbf{2}^+$ and $\mathbf{4}^+$ strongly imply the formation of a mixture of ions, and hence even more IR features.

The second and methodologically more severe aspect concerns the intensities in that none of the computed IR spectra of isomers $\mathbf{1}^+ - \mathbf{21}^+$ shows the strong preference for the band at

1450 cm^{-1} observed in experiment. Similar mismatches of intensities in comparing IRMPD spectra with computational predictions have been noted previously and were mostly assigned to both the nonlinearity of IRMPD and uncertainties in the computational predictions.[17,41,42]

As far as ion structures are concerned, the slight blue shift of the central band in Figure 5a,b by about 25 cm^{-1} to 1470 cm^{-1} in Figure 5c nicely agrees with the theoretical predictions for $\mathbf{9}^+$ (i.e., $\mathbf{2}^+$ and $\mathbf{4}^+$ bear maxima near 1440 cm^{-1}, whereas the maximum for $\mathbf{9}^+$ is at 1470 cm^{-1}). Hence, the IR data imply that a nonnegligible fraction of cycloheptatriene retains the seven-membered ring skeleton upon protonation, even though the ring-protonated toluenes are much more stable. Accordingly, a key question that was left often in the mass spectrometric experiments described above can be resolved by means of the IR features.

Notwithstanding this structural insight gained by means of IRMPD, however, the seemingly simple question for the most favorable protonation site of toluene cannot be answered, because the positions of the major peaks coincide for several isomers, whereas the minor bands and particularly the intensities do not meet the theoretical predictions, thereby preventing to draw definitive structural conclusions. We believe that in this very particular case, the key reason for limited applicability of the method is associated with the strongly multiphotonic character of IRMPD. Thus, for the $C_7H_9^+$ ions studied here, the energetics described above suggest that 10−15 IR photons are required to reach the dissociation threshold. Moreover, given the height of the barrier and the size of the molecule, a notable kinetic shift can be expected to be associated with dehydrogenation.[43] To appreciate a possible influence of multiphotonic processes in the case of $C_7H_9^+$, let us briefly consider the generally accepted view of IRMPD experiments with free electron lasers. After the first photon is absorbed in a given mode ($v_i = 0 \rightarrow v_i = 1$), rapid internal conversion takes place with all other modes $v_{j\neq i}$, thereby making $v_i = 0$ available again for absorption of another photon. This process then repeats until the internal energy of the molecule has reached dissociation threshold. Although population of excited levels of v_i may cause some line broadening, the decisive factor is that no IRMPD can occur at all, if the first photon does not match with an IR absorption feature of the species under study. Therefore, IRMPD intensities show good correlation with linear-IR absorption spectra in many cases.[3,16,17,28,30] However, if the dissociation demands a large number of photons to be absorbed before fragmentation can occur, the multiphotonic nature may well influence the experimentally observed intensities because the IR spectrum is in a sense probed several times before dissociation threshold (E_{thres}) is reached. In the particular case considered here, where also mixtures of isomeric ions come into play, in addition to the mere IR spectra themselves, also the absolute extinction coefficients ($\epsilon_{i,IR}$) may further play a role. Consideration of these arguments would suggest that the measured IRMPD intensities ($I_{i,IRMPD}$) could follow an exponential law, such as $I_{i,IRMPD} = \text{const}\ \epsilon_{i,IR}^n$. In an idealized case, the exponent n is expressed by the fraction $E_{thres}/E_{h\nu}$, which would correspond to $n = 10-15$ for the $C_7H_9^+$ ions studied here. For several reasons, however, primarily the importance of the absorption of the first photon, the non-negligible population of levels other than $v_i = 0$ during ion heating, as well as the initial thermal energy of the reactants, lower values of n are to be expected. Moreover, the previous experience with IRMPD spectra discounts a strongly nonlinear behavior. These objections notwithstanding, the experimental IRMPD spectrum of $C_7H_9^+$ in Figure 5a can be much better modeled with such an exponential approach, e.g., when a 2:1 mixture of the ortho- and para-isomers $\mathbf{2}^+$ and $\mathbf{4}^+$ is assumed in conjunction with $n = 3$. In other words, this crude approach to acknowledge the multiphotonic nature permits us to reproduce the experimental spectrum for a system as reasonably well-known as protonated toluene. In turn, however, if these arguments would hold true also in other systems, the predictive power of IRMPD for unknown compounds must remain somewhat limited, because there exists no straightforward rationale for the estimation of the exponent n (which might in fact be equal to $n = 1$ in many cases). These possible objections notwithstanding, it is to be pointed out that IRMPD has significantly improved the repertoire of methods for the characterization of gaseous ions and is a highly valuable tool for the elucidation of ion structures. Moreover, in particular when the thresholds of the photodissociations sampled are relatively low and thus do not require too many photons, comparison with linear-infrared spectra certainly is more than justified.[44] The difficulties encountered in the specific case of $C_7H_9^+$ ions are thus most likely primarily due to the large number of photons required for fragmentation. For this specific case, consideration of another spectral region (e.g., the C−H stretches at about 3000 cm^{-1})[45] might provide much more definitive insight but could not been achieved with the laser system used.

Conclusions

The structures of $C_7H_9^+$ ions formed upon protonation of toluene is probed by various experimental techniques and complementary theoretical studies. In conjunction with earlier experimental and theoretical findings, it becomes quite clear that protonation initially leads to the ring-protonated isomers which easily interconvert into each other. Isomeric-ion structures are, however, accessible at the elevated internal energies required for ion fragmentation. On the basis of theoretical and labeling data, a mechanistic scheme is suggested that can account for all present and previous experimental observations. Furthermore, the infrared spectra of mass-selected $C_7H_9^+$ ions reveal that a considerable fraction of the ions generated upon protonation of cycloheptatriene retains an intact seven-membered ring. As far as the infrared data are concerned, comparison of the experimental and theoretical spectra suggests a strongly multiphotonic character for the IRMPD spectra of $C_7H_9^+$, which unfortunately hampers a clear-cut assignment of the preferential protonation site.

Acknowledgment. This work was supported by the European Commission, the Deutsche Forschungsgemeinschaft, the Fonds der Chemischen Industrie, and the Grant Agency of the Academy of Sciences of the Czech Republic (No. KJB4040302). D.S. and J.R. particularly thank Joel Lemaire and Philippe Maitre (LCP) as well as the entire staff of CLIO for the productive and always friendly assistance in the measurements using the IR laser.

References and Notes

(1) *IUPAC compendium of chemical technology*, 2nd ed.; Blackwell: Glasgow, 1997; see http://www.iupac.org/goldbook/M03819.pdf.

(2) Solca, N.; Dopfer, O. *Angew. Chem., Int. Ed.* **2002**, *41*, 3628.

(3) Jones, W.; Boissel, P.; Chiavarino, B.; Crestoni, M. E.; Fornarini, S.; Lemaire, J.; Maitre, P. *Angew. Chem., Int. Ed.* **2003**, *42*, 2057.

(4) Ascenzi, D.; Bassi, D.; Franceschi, P.; Tosi, P.; Di Stefano, M.; Rosi, M. *J. Chem. Phys.* **2003**, *119*, 8366.

(5) Schröder, D.; Loos, J.; Schwarz, H.; Thissen, R.; Dutuit, O. *J. Phys. Chem. A* **2004**, *108*, 9931.

(6) Kuck, D.; Schneider, J.; Grützmacher, H.-F. *J. Chem. Soc., Perkin Trans. 2* **1985**, 689.

(7) (a) Mormann, M.; Salpin, J.-Y.; Kuck, D. *J. Eur. J. Mass Spectrom.* **1999**, *5*, 441. (b) Mormann, M.; Kuck, D. *J. Mass Spectrom.* **1999**, *34*, 497. (c) Mormann, M.; Kuck, D. *Int. J. Mass Spectrom.* **2002**, *219*, 497. (d) Salpin, J.-Y.; Mormann, M.; Tortajada, J.; Nguyen, M.-T.; Kuck, D. *Eur. J. Mass Spectrom.* **2003**, *9*, 361. (e) Mormann, M.; Salpin, J.-Y.; Kuck, D. *Int. J. Mass Spectrom.* **2006**, *249*, 340.

(8) Hippler, H.; Reihs, C.; Troe, J. *Z. Phys. Chem.* **1990**, *167*, 1.

(9) Brouwer, L. D.; Mueller-Markgraf, W.; Troe, J. *J. Phys. Chem.* **1988**, *92*, 4905.

(10) Lifshitz, C. *Acc. Chem. Res.* **1994**, *27*, 138.

(11) (a) Kuck, D. *Mass Spectrom. Rev.* **1990**, *9*, 583. (b) Kuck, D. *Int. J. Mass Spectrom.* **2002**, *213*, 101.

(12) Loos, J.; Schröder, D.; Zummack, W.; Schwarz, H.; Thissen, R.; Dutuit, O. *Int. J. Mass Spectrom.* **2002**, *214*, 105.

(13) Trage, C.; Schröder, D.; Schwarz, H. *Organometallics* **2003**, *22*, 693.

(14) Srinivas, R.; Sülzle, D.; Weiske, T.; Schwarz, H. *Int. J. Mass Spectrom. Ion Processes* **1991**, *107*, 368.

(15) For details about such corrections, see refs 5 and 12.

(16) Maitre, P.; Le Caer, S.; Simon, A.; Jones, W.; Lemaire, J.; Mestdagh, H.; Heninger, M.; Mauclaire, G.; Boissel, P.; Prazeres, R.; Glotin, F.; Ortega, J.-M. *Nucl. Instrum. Methods Phys. Res. A* **2003**, *507*, 541.

(17) Le Caer, S. Ph.D. Thesis, Universite Paris-Sud, Orsay, France, 2003.

(18) Vosko, S. H.; Wilk, L.; Nusair, M. *Can. J. Phys.* **1980**, *58*, 1200.

(19) Lee, C.; Yang, W.; Parr, R. G. *Phys. Rev. B* **1988**, *37*, 785.

(20) Miehlich, B.; Savin, A.; Stoll, H.; Preuss, H. *Chem. Phys. Lett.* **1989**, *157*, 200.

(21) Frisch, M. J.; Trucks, G. W.; Schlegel, H. B.; Scuseria, G. E.; Robb, M. A.; Cheeseman, J. R.; Zakrzewski, V. G.; Montgomery, J. A., Jr.; Stratmann, R. E.; Burant, J. C.; Dapprich, S.; Millam, J. M.; Daniels, A. D.; Kudin, K. N.; Strain, M. C.; Farkas, O.; Tomasi, J.; Barone, V.; Cossi, M.; Cammi, R.; Mennucci, B.; Pomelli, C.; Adamo, C.; Clifford, S.; Ochterski, J.; Petersson, G. A.; Ayala, P. Y.; Cui, Q.; Morokuma, K.; Malick, D. K.; Rabuck, A. D.; Raghavachari, K.; Foresman, J. B.; Cioslowski, J.; Ortiz, J. V.; Baboul, A. G.; Stefanov, B. B.; Liu, G.; Liashenko, A.; Piskorz, P.; Komaromi, I.; Gomperts, R.; Martin, R. L.; Fox, D. J.; Keith, T.; Al-Laham, M. A.; Peng, C. Y.; Nanayakkara, A.; Gonzalez, C.; Challacombe, M.; Gill, P. M. W.; Johnson, B. G.; Chen, W.; Wong, M. W.; Andres, J. L.; Head-Gordon, M.; Replogle, E. S.; Pople, J. A. *Gaussian 98*, revision A.11; Gaussian, Inc.: Pittsburgh, PA, 1998.

(22) (a) Williams, D. H.; Hvistendahl, G. *J. Am. Chem. Soc.* **1974**, *96*, 6755. (b) Hvistendahl, G.; Williams, D. H. *J. Chem. Soc., Perkin Trans. 2* **1975**, 881.

(23) Ishikawa, Y.; Yilmaz, H.; Yanai, T.; Nakajima, T.; Hirao, K. *Chem. Phys. Lett.* **2004**, *396*, 16 and references therein.

(24) Dopfer, O.; Lemaire, J.; Maitre, P.; Chiavarino, B.; Crestoni, M. E.; Fornarini, S. *Int. J. Mass Spectrom.* **2006**, *249*, 149.

(25) Loos, J.; Schröder, D.; Schwarz, H. *J. Org. Chem.* **2005**, *70*, 1073.

(26) Derrick, P. J.; Hammerum, S. *Can. J. Chem.* **1986**, *64*, 1957.

(27) Data converted to 0 K and taken from: Lias, S: G.; Hunter, E. P. L. *J. Phys. Chem. Ref. Data* **1998,** *27*, 413.

(28) Simon, A.; Jones, W.; Ortega, J.-M.; Boissel, P.; Lemaire, J.; Maitre, P. *J. Am. Chem. Soc.* **2004**, *126*, 11666.

(29) Oomens, J.; Moore, D. T.; Meijer, G.; von Helden, G. *Phys. Chem. Chem. Phys.* **2004,** *6*, 710.

(30) Dopfer, O.; Solcà, N.; Lemaire, J.; Maitre, P.; Crestoni, M.-E.; Fornarini, S. *J. Phys. Chem. A* **2005,** *109*, 7881.

(31) Dunbar, R. C. *J. Am. Chem. Soc.* **1975,** *97*, 1382.

(32) Ausloos, P. *J. Am. Chem. Soc.* **1982,** *104*, 5259.

(33) Ignatyev, I. S.; Schaefer, H. F., III. *J. Am. Chem. Soc.* **2004,** *126*, 14515.

(34) Data converted to 0 K and taken from: (a) NIST Standard Reference Database Number 69, June 2005 Release, National Institute of Standards and Technology, http://webbook.nist.gov/chemistry/. (b) Lias, S. G.; Bartmess, J. E.; Liebman, J. F.; Holmes, J. L.; Levin, R. D.; Mallard, W. G. Gas-Phase Ion and Neutral Thermochemistry. *J. Phys. Chem. Ref. Data* **1998**, *Suppl. 1*, 17.

(35) Data for neutral C_6H_5 taken from: Berkowitz, J.; Ellison, G. B.; Gutman, D. *J. Phys. Chem.* **1994**, *98*, 2744.

(36) In contrast to a reviewer, we consider it as mandatory to at least explore the structural alternatives of $C_7H_9^+$ ions, because the occurrence of hydrogen as well as carbon scrambling in the dissociation clearly demonstrates that the assumption of an intact toluene structure is insufficient.

(37) (a) Dunbar, R. C. *Int. J. Mass Spectrom. Ion Processes* **1990**, *100*, 423. (b) Van de Guchte, W. J.; Van der Hart, W. J.; De Koning, L. J.; Nibbering, N. M. M.; Dunbar, R. C. *Int. J. Mass Spectrom. Ion Processes* **1993**, *123*, 11.

(38) Ausloos, P.; Lias, S. G.; Buckley, T. J.; Rodgers E. E. *Int. J. Mass Spectrom. Ion Processes* **1998**, *92*, 65.

(39) Bouchoux, G.; Yáñez, M.; Mó, O. *Int. J. Mass Spectrom.* **1999**, *185/186/187*, 241.

(40) Cooks, R. G.; Beynon, J. M.; Caprioli, R. M.; Lester, G. R. *Metastable Ions*; Elsevier: Dordrecht, The Netherlands, 1973.

(41) Moore, D. T.; Oomens, J.; Eyler, J. R.; von Helden, G.; Meijer, G.; Dunbar, R. C. *J. Am. Chem. Soc.* **2005**, *127*, 7243.

(42) Nee, M. J.; Osterwalder, A.; Neumark, D. M.; Kaposta, C.; Cibiran Uhalte, C.; Xie, T.; Kaledin, A.; Bowman, J. M.; Carter, S.; Asmis, K. R. *J. Chem. Phys.* **2004**, *121*, 7259.

(43) Lifshitz, C. *Eur. J. Mass Spectrom.* **2002**, *8*, 85.

(44) Lemaire, J.; Boissel, P.; Heninger, M.; Mauclaire, G.; Bellec, G.; Mestdagh, H.; Simon, A.; Le Caer, S.; Ortega, J. M.; Glotin, F.; Maitre, P. *Phys. Rev. Lett.* **2002**, *89*, 273002.

(45) (a) Solca, N.; Dopfer, O. *Angew. Chem., Int. Ed.* **2003**, *42*, 1537. (b) Solca, N.; Dopfer, O. *J. Am. Chem. Soc.* **2003**, *125*, 1421.